Supporting Information DOI: c6ta08868f

High surface area carbon from polyacrylonitrile for high-performance electrochemical capacitive energy storage

Kishor Gupta,[a] Tianyuan Liu,[b] Reza Kavian,[b] Han Gi Chae,[c] Gyeong Hee Ryu,[c] Zonghoon Lee,[c] Seung Woo Lee,[b] Satish Kumar[a,*]

Method

Sample preparation

The high surface area carbon was manufactured using the following procedure: PAN copolymer (with 6.7% methacrylate) powder (molecular weigh 100,000 g/mole) was first stabilized at 285 ^{o}C for 16 h in a box furnace with an air purge and then air purge was stopped and stabilization was continued at that temperature for another 6h. After stabilization, PAN powder was soaked in aqueous KOH solution (6 M) for 24 h at room temperature followed by drying at 80 ^{o}C. The KOH impregnated dry powder was activated at 800 ^{o}C for 1 h under Argon environment using a heating rate of 5 ^{o}C/min. The activated carbon is referred to as A-PAN in this manuscript.

Characterization

The surface area and pore size distribution analysis for the stabilized and activated PAN materials were done by nitrogen gas adsorption-desorption at 77K using ASAP 2020 (Micromeritics Inc). Before the analysis, the activated PAN materials were degassed at 90 ^{o}C for 16 h. BET (Brunauer, Emmet, and Teller) analysis for surface area and density functional theory (DFT) analysis for pore volume and pore size distribution were conducted.[1-3] Similar process was conducted for commercial activated carbon (YP-50F, Kuraray Chemical Company, Japan, 0.60 cm^3) for comparison.

Electrical conductivities of various electrodes were measured by using Signatone four-point probe (circular sample of half inch diameter, three measurements were taken in the middle by rotating the sample by 60 degrees, and average is reported). SEM LEO 1530 was used for CNT and electrode imaging. Atomic resolution transmission electron microscopy was done using an aberration-corrected FEI Titan Cubed TEM (FEI Titan^3 G2 60-300), operated at 80 kV acceleration voltage with a monochromator. The microscope provides sub-Angstrom resolution at 80 kV and -15 ± 0.5 µm of spherical aberration (C_s). The atomic images were taken using a white atom contrast in order to obtain actual atom positions under properly focused conditions needed for direct image interpretation.

Electrochemical Measurements:

The slurry was prepared by mixing 77 wt% active materials with 11.5 wt% conductive carbon black (super P) as a conducting agent and 11.5 wt% polyvinylidene fluoride (PVDF) dissolved in N-methyl-2-pyrrolidone (NMP) as a binder, which was then coated onto Al foil and dried under vacuum at 70 °C for overnight.

The composite electrodes were prepared by mixing 80 wt% of active materials with 20 wt% of few-walled carbon nanotubes (CNTs, Continental Carbon Nanotechnologies, Inc, ~ 1% catalytic impurity). CNT was directly used as received and sonicated in DMF for 24 h at the concentration of 1 mg/300 mL, and then A-PAN or AC was added to the mixture. After sonicating for 30 min, the dispersion was filtered using cellulose filter paper (1 µm pore size, Whatman RC60). A high pressure (300 MPa) was applied to the electrode for further densifying the electrodes. Before the measurements, the A-PAN electrodes were vacuum dried at 100 ^{o}C for 4 days.

Swagelok cells were used for the electrochemical measurements. The cells were assembled in an Ar-filled glovebox (MBraun) with O_2 level and H_2O level lower than 0.1 ppm. The electrochemical characteristics of the electrodes were evaluated

using Bio-Logic VMP3 potentiostat/galvanostat at room temperature. For the doctor blade methods, the mass loading of active materials used was controlled between 1-3 mg/cm^2. The capacitance was calculated based on the galvanostatic discharge curve by following C=4I/(dV/dt)m, where dV/dt is calculated from the slope of the galvanostatic discharge curve, I is the current, m is the total mass of all electrodes. In symmetric configuration both $EMIMBF_4$ (Sigma Aldrich) and 1 M of $EMIMBF_4$ in acetonitrile were used as electrolytes, the voltage window was 0-3 V. The separator was Celgard 3501. In the asymmetric configuration, pieces of Li metal were used as anode while the carbon-based electrode was used as cathodes, 1 M LiPF6 in ethylene carbonate (EC) and dimethyl carbonate (DMC) (3:7 volume ratio, BASF) was used as electrolyte. The voltage window was controlled between 1.5-4.5 V vs. Li and two pieces of Celgard 2500 were used as separators. The anode test was conducted between 0.01-3 V vs. Li and two pieces of Celgard 2500 were used as separators.

Composite electrodes. In the symmetric configuration, composite electrodes at different mass loadings were used as both cathodes and anodes, 1 M $LiPF_6$ in EC/DMC (3:7 volume ratio) was used as electrolyte, Celgard 3501 was used as separators, the voltage window was controlled between -1.5-1.5 V. In the asymmetric configuration, the voltage window was controlled between 1.5-4.5 V vs. Li, while 2 pieces of Celgard 2500 was used as separators.

Table S1. Surface area and electrochemical performance of various carbon and carbon-based materials as supercapacitors electrode materials.

Materials	Specific surface (area/m^2 g^{-1})	Capacitance (F g^{-1})	Reference
Commercial activated carbons (ACs)	1000–3500	< 100	*Chem. Soc. Rev.*, **2009**, 38, 2520-2531
Particulate carbon from SiC/TiC	1000–2000	100-120	
Functionalized porous carbons	300–2200	100-150	
Carbon nanotube (CNT)	120–500	< 60	
Templated porous carbons (TC)	500–3000	60-140	
Activated carbon fibers (ACF)	1000–3000	80-200	
Carbon cloth	2500	60-100	
Carbon aerogels	400–1000	< 80	
3D porous graphene-based materials	3523	231	*Sci. Rep.,* **2013**, 3.
Pyrolyzed bovine bone	2100	108 ± 9	*Carbon*, **2013**, 55, 291-298
Activated polyacrylonitrile/CNT	1740	302	*Compos Sci. Technol.* **2010***.* 70, 593–598
Carbon fibers	2200	250	*J. Power Sources,* **2008,** *185, 676–684*
SWCNT/polyacrylonitrile composite films	Not available	380	*Carbon,* **2003**, 41, 2427 –2451
SWCNT films	950	85	*ACS Appl. Mater. Interfaces,* **2016***, 8 (37), 24918–24923*
Carbon nanofibers	1162	120	*J. Mater. Chem. A,* **2014**, 2, 418-424
Carbonized agar in the presence of graphene	1200	Not available	*Chem. Commun.,* **2013**, 49, 10427-10429
Functionalized three-dimensional hierarchical porous carbon (THPC)	2870	318.2 in 6 M KOH 224.5 in 1 M $(C_2H_5)_4NBF_4$/AN	*Energy Environ. Sci.,* **2013**, 6, 2497-2504
3D hierarchical porous graphene-like	1810	178 in $TEMABF_4$/PC	*Adv. Mater.* **2013**, 25, 2474-2480
Hyperporous Carbons	4334	Not available	*Adv. Mater.* **2016**, DOI: 10.1002/adma.201603051
Carbonized Al-Based Porous Coordination Polymer	5500	Not available	*J. Am. Chem. Soc.* **2012**, 134, 2864-2867
Activated carbon	4240	Not available	*Ind. Eng. Chem. Res.* **2014**, 53, 15398-15405
Entirely mesoporous carbon nanotube	3802	Not available	*J. Mater. Chem. A,* **2015**, 3, 5148-5161
A-PAN	**3550**	**150 ($EMIMBF_4$)** **216 (1 M $LiPF_6$ in EC/DMC)**	**Our work**
A-PAN/CNT	**Not available**	**180 (1 M $LiPF_6$ in EC/DMC)** **174-304 (Symmetric configuration)**	**Our work**

Table S2. Surface area and porosity analysis for A-PAN and commercial activated carbon YP-50F.

	A-PAN	YP-50F
BET surface area (m^2/g)	3550	1740
DFT pore volume (cm^3/g)	1.78	0.60
Micro pore volume (%)	38	89
Meso pore volume (%)	62	10
Macro pore volume (%)	0	1

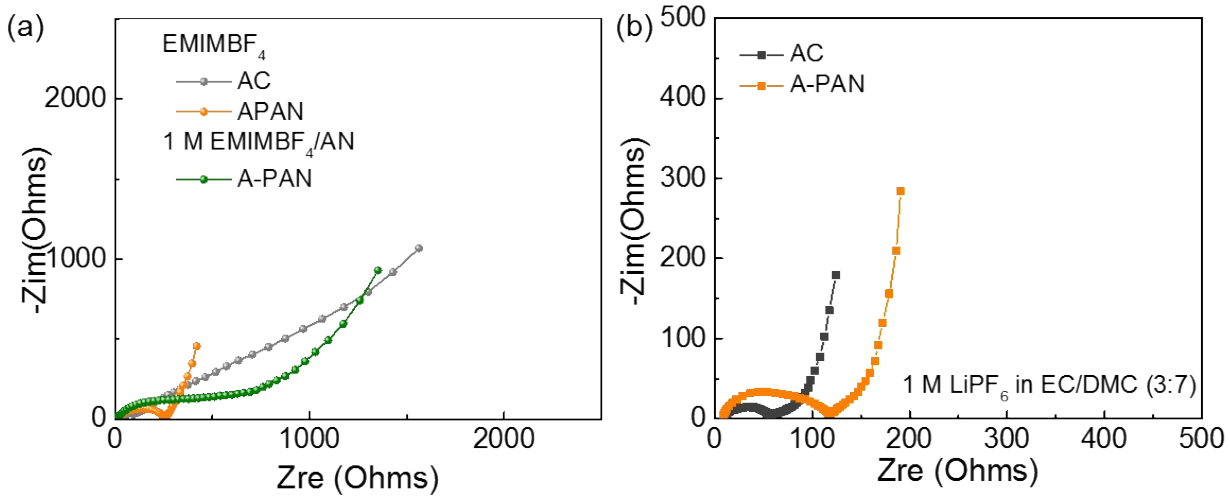

Figure S1. (a) Nyquist plots of symmetric configuration supercapacitors for AC and A-PAN in different electrolytes: 1 M $EMIMBF_4$ in acetonitrile and pure $EMIMBF_4$. (b) Nyquist plots of commercial AC and A-PAN in Li half cells.

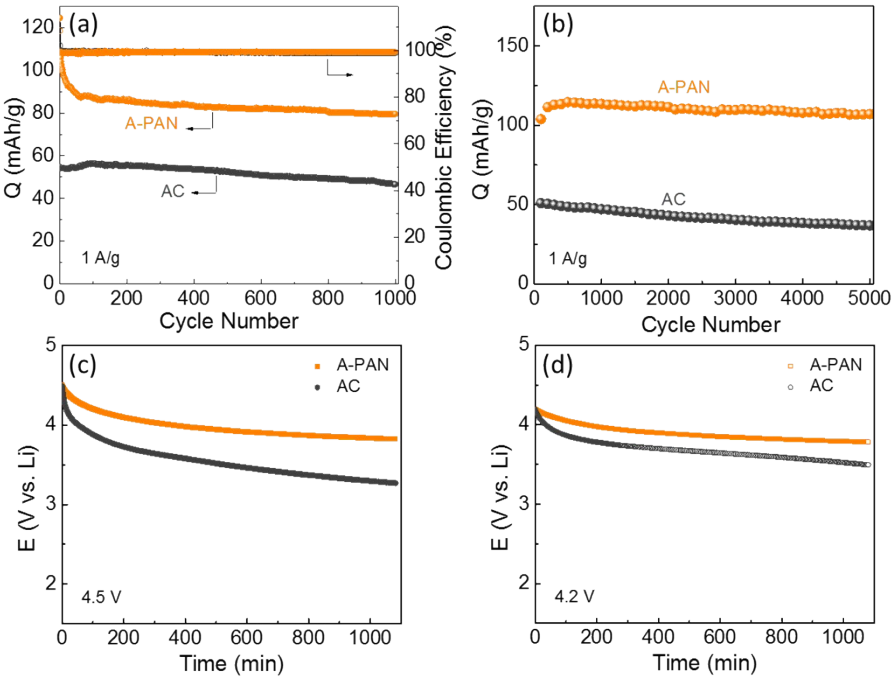

Figure S2. (a) Cycling stabilities and corresponding Coulombic efficiencies of AC and A-PAN electrodes at 1 A/g up to 1,000 cycles. (b) The accelerating cycling stability measurement. Self-discharge test by holding the cell at (c) 4.5 V vs. Li, and (d) 4.2 V vs. Li for 30 min of AC and A-PAN in Li half-cells.

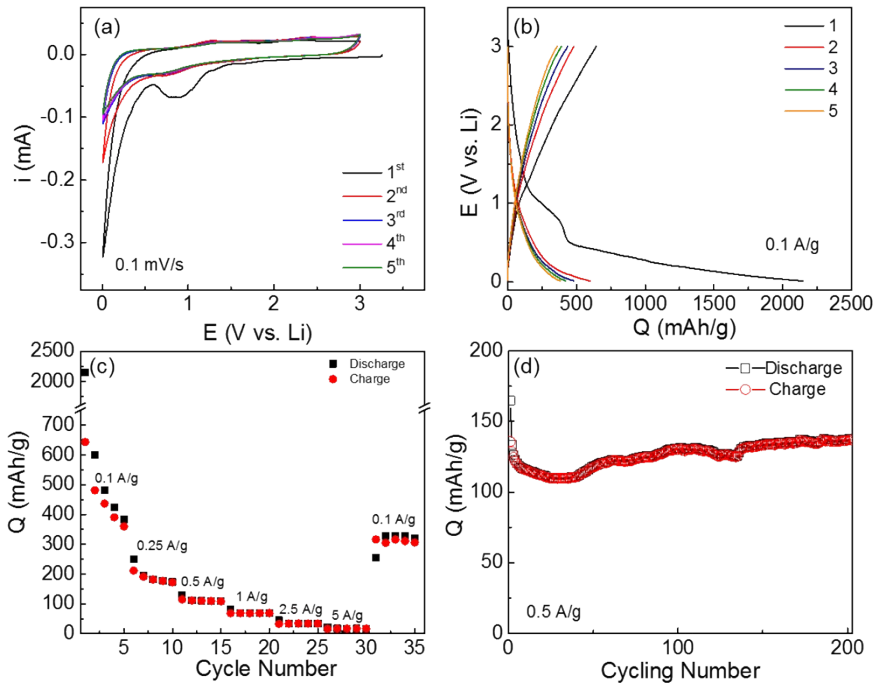

Figure S3. A-PAN anode test, (a) CV scans of A-PAN between 0.01 -3 V vs. Li at a scan rate of 0.1 mV/s. (b) Galvanostatic charge and discharge profiles at 0.1 A/g. (c) Rate-dependent galvanostatic charge and discharge capacities of A-PAN. (d) Cycling stabilities of A-PAN up to 200 cycles at 0.5 A/g.

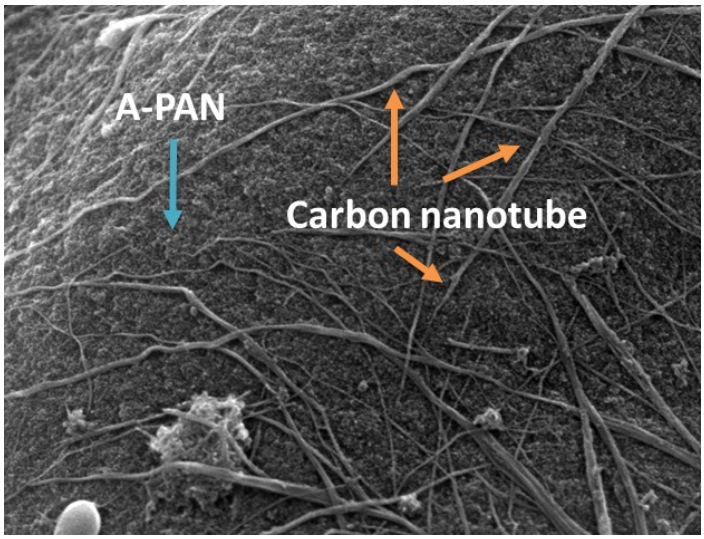

Figure S4. (a) Scanning electron microscope (SEM) image of composite electrodes consist of A-PAN and carbon nanotubes (CNTs) (A-PAN/CNT).

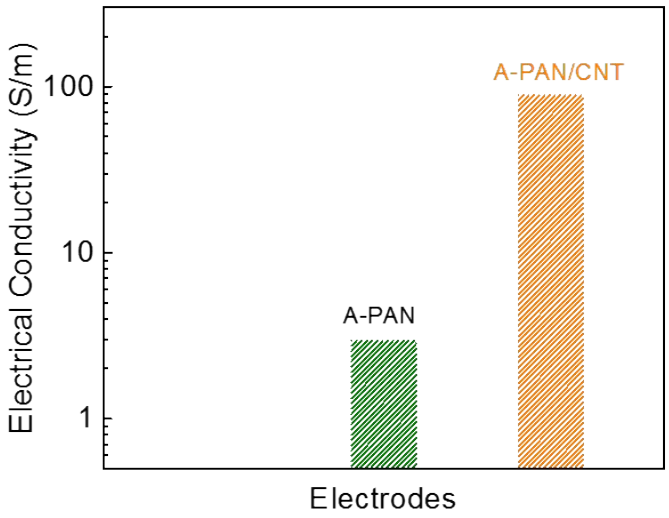

Figure S5. Comparison of in plane electrical conductivity of A-PAN powder and composite electrodes, A-PAN/CNT, made of A-PAN powder and CNT at a mass ratio of 80:20.

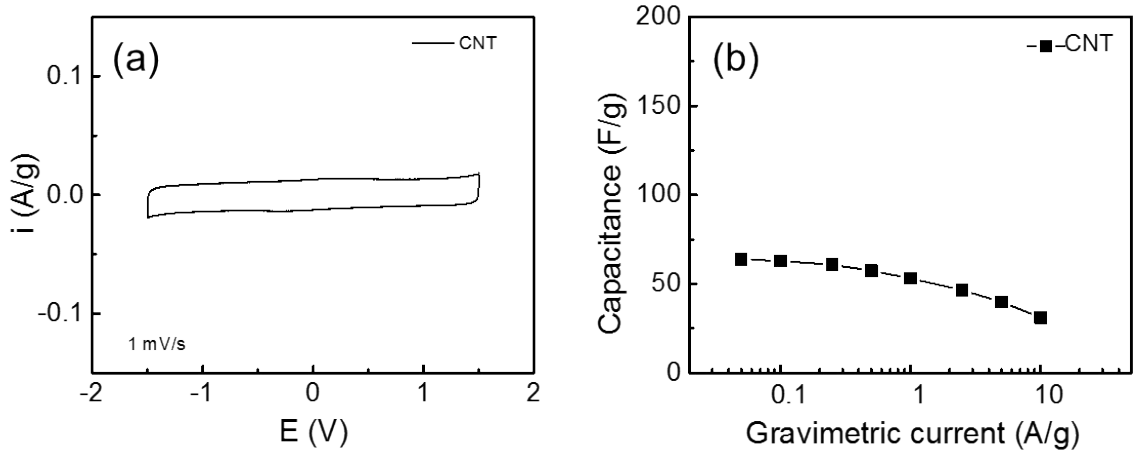

Figure S6. Electrochemical performance of the pristine CNT film based symmetric capacitors using 1 M $LiPF_6$ in ethylene carbonate (EC) and dimethyl carbonate (DMC) (3:7 volume ratio) as electrolyte.

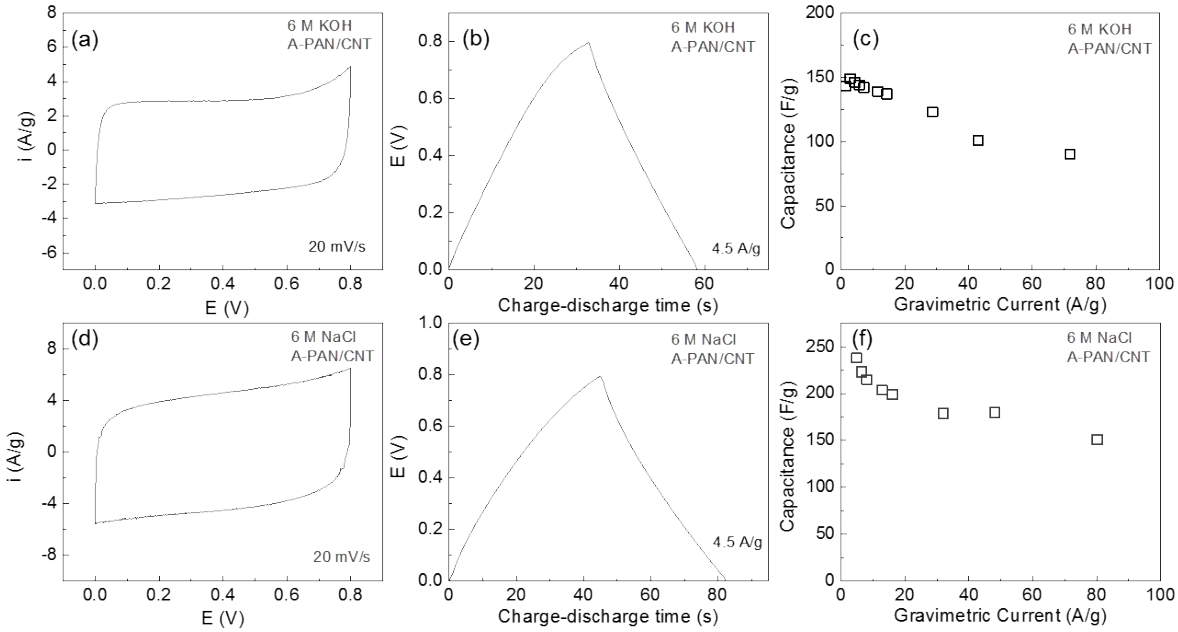

Figure S7. Electrochemical performance of composite electrode, A-PAN/CNT in aqueous electrolytes, (a-c) 6 M KOH, (d-f) 6 M NaCl, the voltage window was between 0-0.8 V using symmetric configuration.

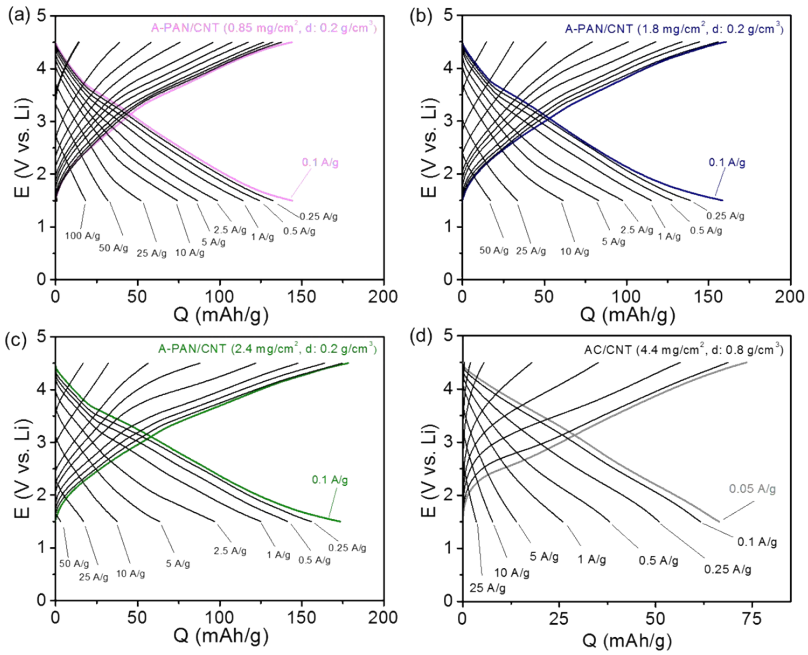

Figure S8. A-PAN/CNT cathode test. Rate-dependent galvanostatic charge/discharge profiles of various composite electrodes, (a-c) the A-PAN/CNT and (d) AC/CNT with varying bulk and mass loading in the range of 1.5-4.5 v vs Li in $LiPF_6$ and EC:DMC in Li cells. Prior to charge and discharge, the cells were held at a constant voltage of 1.5 and 4.5 V versus Li for 30 minutes, respectively.

References:

1. S. Lowell, J. E. Shields, M. A. Thomas and M. Thommes, *Characterization of porous solids and powders: Surface area, pore size and density*, Kluwer Academic Publishers, Dordrecht/Boston/London, 2004.
2. K. S. W. Sing, D. H. Everett, R. A. W. Haul, L. Moscou, R. A. Pierotti, J. Rouquerol and T. Siemieniewska, *Pure & Appl. Chem.*, 1985, **57**, 603.
3. P. A. Webb and C. Orr, *Analytical Methods in Fine Particle Technology*, Micromeritics Instruments Corp., Norcross, Georgia, USA, 1997.